

# 3D detection zone: positioning of electro-sensitive protective equipment (ESPE)

## Determination of the separation distance based on DIN EN ISO 13855

Subcommittee Machinery, Robotics and Automation, Date: 08.01.2026

This Fachbereich AKTUELL provides information to manufacturers and users of machines whose hazardous movements are safeguarded by electro-sensitive protective equipment (ESPE) with a three-dimensional (3D) detection zone, e.g. camera systems or 3D laser scanners.

DIN EN ISO 13855 covers the positioning of safeguards regarding the approach of the human body and in particular the required separation distances between the safeguard and the hazard zone. The standard covers ESPE with one-dimensional or two-dimensional detection zones (light barriers, light curtains, 2D laser scanners) and clearly describes their positioning.

3D systems with volumetric detection are mentioned in the current edition of DIN EN ISO 13855:2025-10 [2], but particular aspects regarding the positioning of 3D detection zones are not specified.

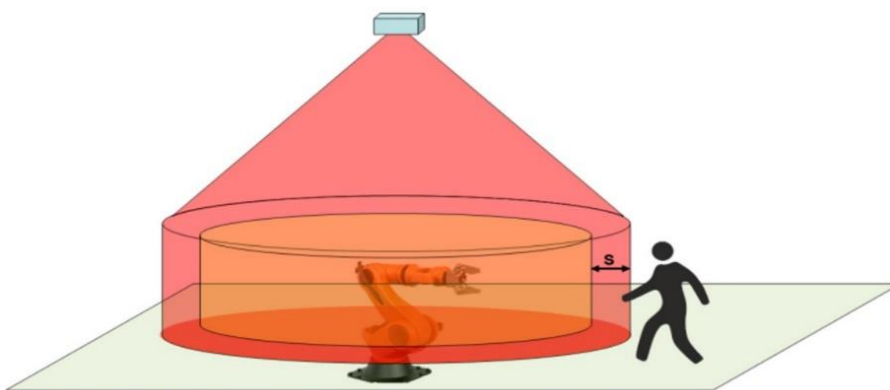


Figure 1 – A 3D ESPE (blue) installed above the robot monitors a cylindrical 3D detection zone (red) with a cone attached above

In the scope of a joint project of FBHM (Fachbereich Holz und Metall) and IFA (Institut für Arbeitsschutz), a typical assembly work process was simulated by using virtual reality and examined with test subjects. The temporally separated collaboration of an operator with a turntable and a robot was safeguarded by a 3D ESPE. The test results provide information on the practical application of DIN EN ISO 13855 regarding 3D detection zones. Within a scope extension of the project, the potential for bypassing detection zones was examined.

# Table of contents

<b>1</b>	<b>Separation distances for three-dimensional detection zones</b> .....	<b>2</b>
<b>2</b>	<b>Example of the adaptation of the rules from DIN EN ISO 13855 for a 3D detection zone</b> .....	<b>3</b>
2.1	Separation distance $S$ .....	4
2.2	Reaching distance through a detection zone $D_{DT}$ .....	6
2.3	Application to the example .....	6
2.4	Spherical 3D detection zone.....	7
2.5	Conical/pyramidal 3D detection zone .....	7
2.6	Recommendations .....	8
<b>3</b>	<b>Design recommendations for 3D detection zones and their marking</b> .....	<b>8</b>
<b>4</b>	<b>Ground clearance of detection zones and 3D detection zones</b> .....	<b>9</b>
<b>5</b>	<b>Investigations by IFA</b> .....	<b>9</b>
5.1	Project IFA 5116 .....	9
5.2	Project IFA 5125.....	10
<b>6</b>	<b>Summary and limits of application</b> .....	<b>11</b>

## 1 Separation distances for three-dimensional detection zones

The methods for determining the required separation distance between the position of an ESPE and the hazard zone in accordance with DIN EN ISO 13855 can basically be applied to 3D detection zones as well. In some cases, however, they need to be adapted or extended.

Supplemental distance factors are described in Annex AA of DIN EN IEC 61496-3 [3] and DIN IEC/TS 61496-4-3 [5] as well as in section 5.6 of DIN EN ISO 13855:2025-10 [2].

The supplemental distance factor  $d$  in [2] represents an exception as it considers that, for technical reasons, an object or a part of the human body to be detected must have entered the 3D detection zone partially or completely to be reliably detected.

Some particularities must be considered in practical application. The direction of approach for example does not refer to the orientation of the 3D detection zone, but to the boundary surface oriented towards the operator. According to DIN EN ISO 13855:2025-10, section 7, the direction of approach of the person must consider the boundary surface of a 3D ESPE that limits the 3D detection zone at the point of detection. With a 3D detection zone design that is adequately adapted to the shape and position of the hazard zone, it is no longer possible to reach around, over or under it.

The walking speed of 1600 mm/s specified in the standard is also assumed for 3D detection zones.

The separation distances for three-dimensional detection zones (3D) can basically be determined using the same methods as for two-dimensional detection zones (2D).

For lidar systems (3D AOPDDR), the requirements of DIN EN IEC 61496-3 must be observed. Annex AA of the 4th edition, issue 2025 [4], already considers important changes to DIN EN ISO 13855:2025-10. This applies in particular to application-dependent supplemental distance factors that must be considered in the basic formula for the separation distance. This aspect is explained in more detail in chapter 2.1. For stereo-based 3D systems, the aspects described in Annex AA of DIN IEC/TS 61496-4-3 apply in addition.

In contrast to the 2010 edition of DIN EN ISO 13855 [1], the above-mentioned standards also consider a detection capability within a range of 40 mm to 55 mm. This is of particular importance for 3D safeguards.

## 2 Example of the adaptation of the rules from DIN EN ISO 13855 for a 3D detection zone

Distances to hazardous areas when using ESPE are usually determined in accordance with DIN EN ISO 13855. However, the standard does not provide specific instructions for the positioning of 3D detection zones when these are implemented, for example, as camera systems or 3D laser scanners. Therefore, the following example with an industrial robot demonstrates how the rules of the standard can be applied to a 3D detection zone.

A 3D ESPE which is mounted above the robot monitors a cylindrical 3D detection zone (see Figure 1). A **separation distance  $S$**  must be maintained between the hazard zone (orange) and the operator.

The cylindrical 3D detection zone should not extend to the floor, as it should not be recognised as an 'obstacle'. Measurement tolerances of a 3D ESPE in position measurement require that a certain distance from the surrounding area must always be maintained to achieve sufficient availability.

If the height  $H_{DB}$  of the detection zone above the reference plane exceeds 200 mm, there is always a risk of undetected access underneath the detection zone. This must be considered in the risk assessment (see chapter 4).

The radius of the cylinder with the robot at its centre corresponds to the radius of the hazard zone that can be reached by the robot, and which is also assumed to be cylindrical (shown in orange in Figure 1). The **separation distance  $S$**  must be added.

The cone attached from the upper boundary surface of the cylinder to the 3D ESPE must be added to the 3D detection zone, as the intrusion of extended objects into this area must be considered as violation of the 3D detection zone. Otherwise, no detection would be possible in the configured 3D detection zone in the hidden detection area below these objects.

The cylindrical 3D detection zone with a cone as the reference geometry was selected on the basis of design recommendations (see chapter 3). This allows the advantages provided by the 3D detection zone which is adapted to the shape of the danger zone to be implemented.

This geometry is compared with a spherical and a conical 3D detection zone in chapter 2.4 and 2.5.

## 2.1 Separation distance S

The following explanations consider the new terms and formulas used in DIN EN ISO 13855:2025-10. For calculating the separation distance S, previously referred to as minimum distance, table 1 compares the basic formula (17) and formula (AA.4) for camera systems with orthogonal approach to a detection zone.

Table 1 – Formulas and elements for calculating the separation distance

Basic formula (17) from DIN EN ISO 13855:2025-10 adapted for “reaching through” $S = (K \times T) + D_{DT} + Z$	Formula (AA.4) from DIN IEC/TS 61496-4-3 [in accordance with DIN EN ISO 13855:2010-10] $S_o = (K \times T) + C_{tz} + d$ $[S = (K \times T) + C]$
<p><u>New terms and formula symbols in accordance with DIN EN ISO 13855:2025-10:</u></p> <p><b>S</b> Separation distance, i.e. calculated minimum distance between the position of the ESPE and the hazard zone</p> <p><b>D<sub>DS</sub></b> Reaching distance associated with ESPE (<math>D_{DS} = \max(D_{DO}, D_{DT}, D_{DU})</math>)</p> <p><b>D<sub>DO</sub></b> Reaching distance over a detection zone (reaching over))</p> <p><b>D<sub>DT</sub></b> Reaching distance through a detection zone (reaching through)</p> <p><b>D<sub>DU</sub></b> Reaching distance under a detection zone (reaching under)</p> <p><b>Z</b> Depending on the application, supplemental distance factor, including:</p> <p><b>Z<sub>G</sub></b> Supplement for general measurement errors, e. g.:</p> <p><b>Z<sub>P</sub></b> Position uncertainty of the operator, depending on the measurement accuracy of the ESPE</p> <p><b>Z<sub>M</sub></b> Position uncertainty of the machinery, depending on the measurement accuracy of the machine position measuring system</p> <p><b>Z<sub>R</sub></b> Reflection-based measurement errors, if a retroreflector is in the vicinity of an ESPE</p> <p><b>Z<sub>F</sub></b> Supplement for lack of ground clearance of moving machinery (e.g. a vehicle)</p> <p><b>Z<sub>B</sub></b> Supplement for the decreasing braking torque of moving machinery (e.g. a vehicle)</p> <p><b>d<sub>e</sub></b> Effective detection capability: Sensing function parameter limit set by the manufacturer or the integrator of the ESPE</p>	<p><u>Terms and formula symbols known according to DIN EN ISO 13855:2010-10:</u></p> <p><b>S</b> Minimum distance, i. e. calculated distance between the ESPE and the hazard zone</p> <p><b>K</b> Approach speed of the body or parts of the body</p> <p><b>T</b> Overall system response time</p> <p><b>d</b> Detection capability: ability to detect the specified test pieces in the specified detection zone. The dimensions of the test piece correspond largely to the minimum detectable object size.</p> <p><b>C<sub>tz</sub></b> Device-specific distance factor for position uncertainty in the localisation of parts of the human body (to be indicated by the manufacturer in accordance with DIN IEC/TS 61496-4-3)</p> <p><u>Replaced terms and formula symbols:</u></p> <p><b>C</b> Intrusion distance into the hazard zone</p> <p><b>C<sub>Ro</sub></b> Intrusion distance when reaching over</p> <p><b>C<sub>Rt</sub></b> Intrusion distance when reaching through</p>

Supplemental distance factors depending on the application, device measurement errors and position uncertainties were not described in DIN EN ISO 13855:2010-10 and must therefore be considered when adapting to 3D detection zones depending on the application and the 3D technology applied:

$$Z = Z_G + Z_R + Z_F + Z_B + d \quad | \quad Z_G = Z_P + Z_M$$

Comparing the old and new formula symbols:  $C = D_{DT}$  and  $(C_{tz} + d) = Z$ .

The supplemental distance factors  $Z_P + d$  and  $C_{tz} + d$  in the respective formula consider the fact that human body parts must be detected with sufficient probability and, in the worst case, can only be reliably detected if they have partially or completely entered the 3D detection zone.

For the sake of clarity and considering the relevance in this document, only the supplemental distance factors for  $Z_P + d$  are applied in the calculation examples.

**Notes:**

The effective detection capability  $d_e$  is frequently determined by the minimum detectable object size  $d$  and, depending on the technology, in addition by e.g. the shape and reflectivity of the object.

A better detection capability means that a smaller object can be detected.

The supplier may specify several values for the minimum detectable object size, for example, range-dependent values.

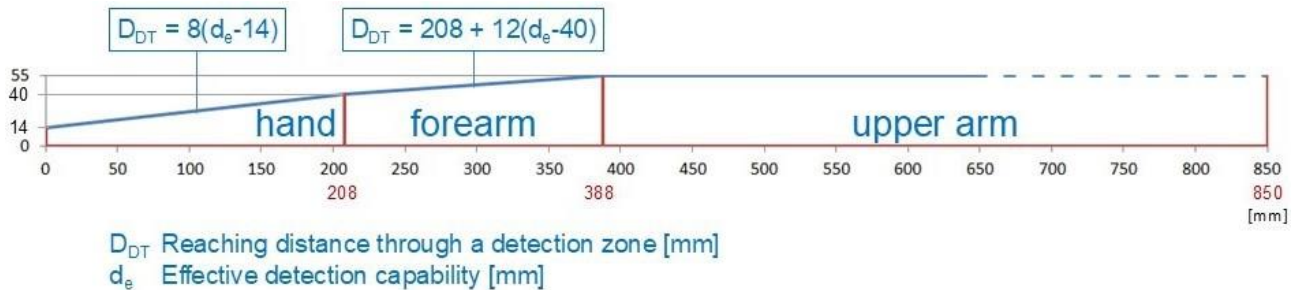


Figure 2 – Reaching distance  $D_{DT}$  and detection capability  $d_e$ .  
 Correlation according to DIN EN ISO 13855:2025-10, Figure G.3

Since the  $K \times T$  proportion is independent of the 3D detection zone geometry, this aspect is not considered in the following.  $S$  denotes the separation distance including the supplemental distance factors described above.

DIN EN ISO 13855:2025-10 provides two different calculation methods for  $S$ , depending on the direction of approach, orthogonal or parallel to the detection zone.

For a 3D detection zone, the smaller of the two values can be used for the separation distance  $S$ .

**Notes:**

Since the described cylindrical 3D detection zone extends both in the direction of approach to the hazard zone and orthogonal to it (corresponds to the tangential boundary area of the 3D detection zone), both methods described in DIN EN ISO 13855:2025-10 are applicable at first view (see section 8 'Orthogonal approach to a detection zone' and section 9 'Parallel approach to a detection zone').

According to the flow chart in Figure 1 of DIN EN ISO 13855:2025-10, the possibility of bypassing must always be considered when using ESPE. Chapter 8.2 of the standard provides detailed information on preventing reaching over a vertical detection zone.

When reaching over a horizontal detection zone, a reaching distance factor of  $D_{DS} = 1200$  mm must be considered, depending on  $H_D$  with the arm outstretched and the upper body bent.

With reference to Table 2 of the standard, it is therefore recommended to set the upper edge of the cylindrical 3D detection zone proportion  $H_{DT}$  as high as possible.

This always ensures that, regardless of the height  $H_H$  of the hazard zone above the ground, the reaching distance  $D_{DO}$  (when reaching over the detection zone) is smaller than  $D_{DT}$ . Considerations to reaching over should not result in an increase in the separation distance.

Requirements for preventing crawling beneath a detection zone are specified in sections 4.5 and 9.2 for whole-body access. To reduce the risk of reaching under a detection zone, the reaching distance  $D_{DU}$  is specified in sections 8.4.2 and 8.4.3.

## 2.2 Reaching distance through a detection zone $D_{DT}$

Figure 2 is used as the basis for calculating the *reaching distance*  $D_{DT}$  in the case of reaching through a vertical detection zone.  $D_{DT}$  is directly incorporated into the value of the *separation distance*  $S$ .

The geometries selected as examples were analysed for three typical detection capabilities. The results are summarised in Table 2.

### a) Effective detection capability $d_e = 55$ mm

For  $d_e = 55$  mm, a detection of the upper arm from the elbow upwards is typically possible. This detection capability is considered in DIN EN ISO 13855:2025-10 in section 8.3.3 in the range of  $40 \text{ mm} < d_e \leq 55 \text{ mm}$ . Using formula

$$D_{DT} = 12(d_e - 40) \text{ mm} + 208 \text{ mm}$$

results in a reaching distance for the forearm, including the outstretched hand, of  $D_{DT} = 388$  mm.

### b) Effective detection capability $d_e = 70$ mm

For  $d_e = 70$  mm, an arm cannot be detected reliably. Therefore, according to DIN EN ISO 13855:2025-10, section 8.3.4, a reaching distance of  $D_{DT} = 850$  mm must be considered in the range of  $55 \text{ mm} < d_e \leq 120 \text{ mm}$ .

### c) Effective detection capability $d_e = 200$ mm

The value 200 mm is specified in DIN EN IEC 61496-3 and DIN IEC/TS 61496-4-3 as the maximum diameter of a test piece for safe body detection. Accordingly, a reaching distance for the arm of  $D_{DT} = 850$  mm must also be assumed in this case.

## 2.3 Application to the example

For the example of the cylindrical 3D detection zone shown in Figure 1, the application of DIN EN ISO 13855:2025-10 gives the following results for the three detection capabilities considered.

The following typical assumptions were made for the calculation examples:

- The **supplemental distance factor  $d$**  for the minimum detectable object size corresponds to the individual effective detection capability  $d_e$  under consideration.
- $K = 1600$  mm/s (walking speed);  $T = 0,3$  s;  $Z_P = 50$  mm

### a) For $d_e = 55$ mm

results  $D_{DT} = 388$  mm (forearm with hand outstretched).

Verifying whether  $D_{DO} > D_{DT}$  according to the procedure described above leads to the conclusion that, from a height  $H_{DT}$  of the upper edge of the cylindrical 3D detection zone proportion of 2200 mm,  $D_{DO}$  assumes a maximum value of 250 mm and no increase results.

Thus, in the selected example

$$S = (K \times T) + D_{DT} + Z_P + d_e = 973 \text{ mm}$$

### b) For $d_e = 70$ mm

results  $D_{DT} = 850$  mm (outstretched arm). Thus, in the selected example

$$S = (K \times T) + D_{DT} + Z_P + d_e = 1450 \text{ mm}$$

From a height  $H_{DT}$  of 1400 mm at the upper edge of the cylindrical 3D detection zone proportion, there is no increase due to possible reaching over.

### c) For $d_e = 200$ mm

results  $D_{DT} = 850$  mm (outstretched arm). Thus, in the selected example

$$S = (K \times T) + D_{DT} + Z_P + d_e = 1580 \text{ mm}$$

From a height  $H_{DT}$  of the upper edge of the cylindrical 3D detection zone proportion of 1400 mm, there is no increase in this case either due to possible reaching over.

A significant difference in the *separation distance*  $S$  only occurs at the transition from  $d_e = 70$  mm to  $d_e = 55$  mm. In this case, only the forearm including the outstretched hand must be considered as reaching distance  $D_{DT}$  instead of the outstretched arm.

Between  $d_e = 70$  mm and  $d_e = 200$  mm, the difference is small, as the outstretched arm is assumed in both cases.

Table 2 – Results for typical detection capabilities according to chapter 2.2 and 2.3

Detection capability $d_e$	Reaching distance $D_{DT}$	Separation distance $S$
a) 55 mm	388 mm	973 mm
b) 70 mm	850 mm	1450 mm
c) 200 mm	850 mm	1580 mm

### 2.4 Spherical 3D detection zone

A spherical 3D detection zone with a cone attached above represents the detection zone with the smallest volume for single point or spherical hazard spots at a given *separation distance*  $S$ . Compared to the cylindrical 3D detection zone, however, the additional space gained in the leg and head area is hardly relevant in practice. Due to the measurement tolerances mentioned above, a distance  $H_{DB}$  of maximum 200 mm or 300 mm from the floor must be maintained in any case, depending on the result of the risk assessment (see chapter 4). Unintentional violation of the 3D detection zone with the tip of the foot is unlikely with either geometry. Significant differences are only conceivable in very specific applications.

### 2.5 Conical/pyramidal 3D detection zone

A conical or pyramidal 3D detection zone best reflects the optical display options of a 3D ESPE with a fixed opening angle.

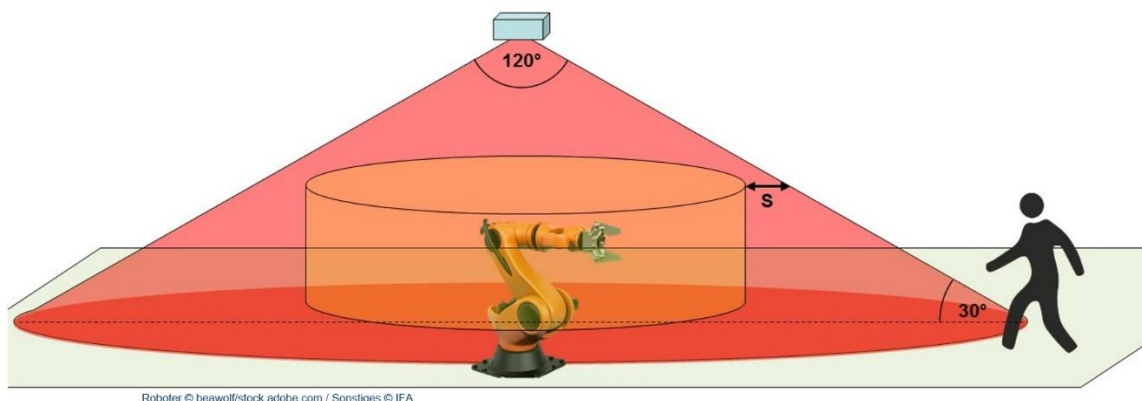


Figure 3 – Illustration of the opening angle of the 3D ESPE and the angle between the 3D detection zone and the approach direction in the limit case of 30°

DIN EN ISO 13855:2025-10 stipulates in section 7 that, in the case of an “oblique” approach direction in relation to the detection zone, an angle of more than 30° is to be assumed to be an orthogonal approach. Referring to a 3D ESPE installed above the hazard zone and aligned vertically downward, the limit case of 30° corresponds to an opening angle of 120° (see Figure 3). Advantages in comparison to a cylindrical geometry are usually not to be expected.

**Note:**

3D ESPE with an opening angle of more than 120° are currently rather unrealistic. Since it can be assumed with the cone geometry that an intruding body will first be detected at the leg, it makes no sense to consider a detection capability of  $d_e = 55$  mm (detection of the arm). For  $d_e = 70$  mm and  $d_e = 200$  mm, the outstretched arm must be assumed, as with the cylindrical 3D detection zone, and no other separation distances result. In operational practice, “leading” detection in the leg area will probably lead to increased unwanted violations of the detection zone (and thus to an incentive for manipulation) or to a greater distance being maintained.

## 2.6 Recommendations

In summary, the following recommendations can be derived from the above considerations:

1. The cylinder geometry with a cone attached above is a good compromise between an easy-to-configure geometry and a good adaptation to the shape of the hazard zone.  $S$  can be calculated with little effort. Sphere or cone do not offer any advantages that justify the increased effort involved in calculating  $S$ , unless such a configuration is supported by a convenient tool, such as e.g. a configuration software.
2. The height  $H_{DT}$  of the cylinder top edge above the floor should be at least 2400 mm for  $d_e > 55$  mm, otherwise 1400 mm are sufficient. Thus, the possibility of reaching over does not lead to an increase in  $S$ , regardless of the height  $H_H$  of the hazard zone.
3. A significant reduction in  $S$  results for  $d_e \leq 55$  mm, while a detection capability of 70 mm compared to 200 mm offers little advantage.
4. The *separation distance*  $S$ , including all supplemental distance factors, is to be calculated as follows:

$$S = (K \times T) + D_{DT} + Z \quad | \quad Z = Z_G + Z_R + Z_F + Z_B + d$$

## 3 Design recommendations for 3D detection zones and their marking

Studies conducted by Fachbereich Holz und Metall and IFA revealed that there are significant individual differences in how people deal with hazard zones: cautious operators tend to avoid violations of the detection zone by maintaining an additional distance from the 3D detection zone boundary. Other operators optimise routes and processes and even accept violations of the 3D detection zone if this does not significantly impact productivity. The key aspect is to take the advantages of 3D technology through flexible adaptation to working conditions and ergonomic design. This includes a proper adaptation of the 3D detection zone as closely as possible to the shape of the hazard area and avoiding ‘corners and edges’ that protrude into the intuitive walking path or working area. The three-dimensional design option allows minimisation of the 3D detection zone size in relation to the hazard zone through flexible design of the detection zone shape. Thus, work processes remain largely unaffected and the incentive to bypass the system is minimised.

The IFA study also provides information that, where possible, 3D detection zones should also be marked at height to prevent 3D detection zone violations. Floor markings may not be sufficient for orientation. The study also showed that a combination of floor markings and warning areas is effective in preventing 3D detection zone violations (see chapter 5).

## 4 Ground clearance of detection zones and 3D detection zones

The edition of DIN EN ISO 13855:2010-10 permitted in section 6.2.2 a maximum height of the detection zone of 300 mm above the reference level (floor).

DIN EN ISO 13855:2025-10 additionally provides the following for the maximum height of detection zones above the reference level:

If an ESPE is used exclusively to detect whole-body access, the height of the detection zone  $H_{DB}$  must not exceed 200 mm. In industrial environments, the possibility of crawling underneath must always be taken into account, and a maximum height  $H_{DB}$  of 300 mm is only permissible if the results of the risk assessment show that this is sufficient.

In a field test with 43 schoolchildren aged at least 14 years, the possibility of bypassing detection zones was examined in more detail. The evaluation of the results clearly shows that even with invisible detection zones it is easily possible to crawl underneath a height of 300 mm over a length of 2000 mm and thus to bypass (see chapter 5).

## 5 Investigations by IFA

### 5.1 Project IFA 5116

The IFA 5116 project 'Protective devices with 3D detection zones on machines: Verification of safety distances using VR methods' was initiated by the MHHW expert committee (now part of FB Holz und Metall) and deals with the determination of safety distances for 3D ESPE: Are the existing normative rules for two-dimensional detection zones transferable? How does the lack of visibility of the 3D detection zone affect this?

Introductory research revealed that the normative reach and step speeds (for normal, non-reflex movements) are based in part on empirical studies conducted a long time ago, mainly at insertion workstations, e.g. presses. Recent normative additions concerned regulations on reaching over or on obstacles in the way. In the standardisation of 3D ESPE, the forearm is modelled as a truncated cone.

The project was carried out in mixed reality at the IFA's SUTAVE laboratory [6]. The methodology offers the following advantages: there are no real hazards, motion tracking with automatic data collection is possible, scene changes are easy to implement and the ESPE properties are adjustable. The scene depicted a collaborative workstation where the test subjects performed a pattern recognition task and an assembly task on a real turntable with a virtually displayed robot.

The study specified two 3D detection zone geometries (sphere and cuboid) and three marking types (without marking, floor marking, warning zone). Movement data (3D detection zone violations, walking paths, movement and working speed), quality measures (pattern recognition and reproduction) and stress (questionnaires) were collected. Twenty test subjects each completed two runs (both geometries) of 20 work cycles each.

The study results confirm the basic suitability of mixed reality as a method. The stress levels determined during task performance show no significant differences between the different marking forms. Even the maximum walking speed per cycle does not differ significantly. The normatively assumed walking speed of 1600 mm/s is confirmed. This also applies to the speed of the hands, which serves as a reference for the assumed gripping speed (2000 mm/s).

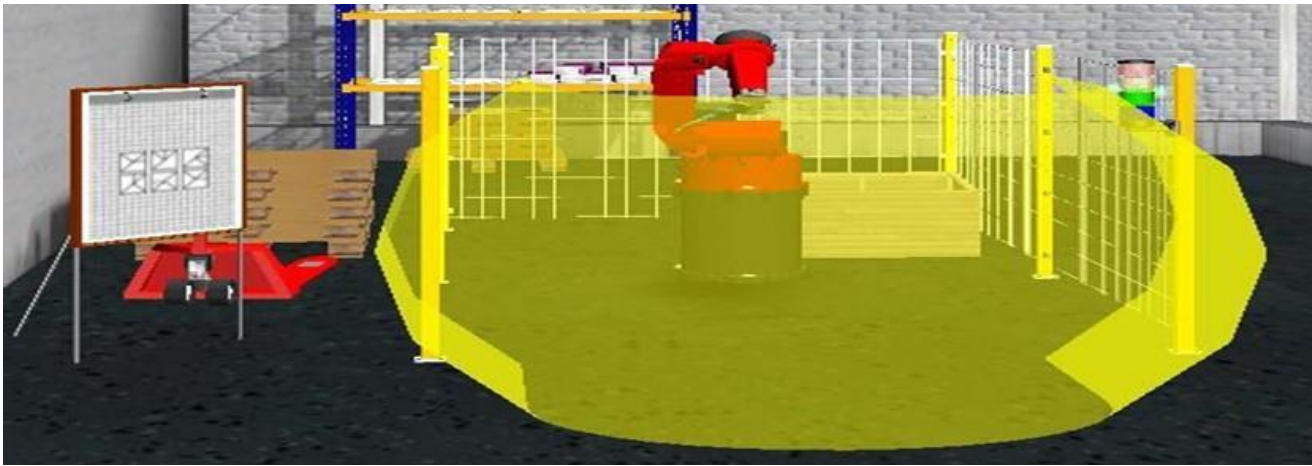


Figure 4 – Test setup in virtual reality without the actual work equipment (e.g. turntable, assembly frame, material deposit). The transparently displayed 3D detection zone was not visible to the test subjects.

Regarding the 3D detection zone geometries, the sphere causes significantly fewer 3D detection zone violations than the cuboid. This can be attributed to its smaller volume and the absence of 'corners and edges'. The 'warning zone' marking resulted in fewer 3D detection zone violations than the 'no marking' and 'floor marking' variants. This is indicative for the effectiveness of an upstream warning zone.

In the case of the cuboid, there was a concentration of 3D detection zone violations at the edges, both without marking and with a warning zone. With floor marking, the 3D detection zone was violated more evenly at the front. This result suggests that the test subjects were unable to correctly interpolate the 3D detection zone upwards from the floor marking.

In general, there is a high degree of inter-individual variance in the number of 3D detection zone violations, which indicates that there are significant individual differences in risk tolerance. Further information can be found in the pilot study „Gestaltungsanforderungen an dreidimensionale Schutzräume für Fertigungszellen mit Mensch-Roboter-Interaktion“ [7] and is linked on the IFA 5116 project website (<http://www.dguv.de/ifa>, web code d105325).

## 5.2 Project IFA 5125

The supplement to project IFA 5116 by project IFA 5125 „Schutzeinrichtungen mit 3D- Schutzräumen an Maschinen: Überprüfung der Unterkriechbarkeit“ was carried out in a preliminary study with ten adult IFA employees and a field study with 43 school test subjects. The scope of DIN EN ISO 13855 refers to persons aged 14 years or older.

The test results therefore refer to the most unfavourable application case covered by the standard in terms of body measurements.

The measured group of 43 test subjects in the main study is representative of the age group under consideration in terms of body height and waist circumference.

Almost all participants (41 out of 43) were able to crawl beneath  $H_{DB} = 300$  mm. Even  $H_{DB} = 250$  mm did not pose an obstacle for the majority (30 out of 41). Only when the height was reduced to  $H_{DB} = 200$  mm, just one test person succeeded.

The length of the detection zone (the length of the distance to be crawled beneath) has a significantly weaker influence on the "ability to crawl underneath" than the height. Although detection zone violations are more frequent and longer at a detection zone length of 2000 mm than at 200 mm, the initial positions of the detection zone violations in the crawling direction, however, do not show any discernible regularities. There are no indications of a 'critical length' of the detection zone beyond which detection zone violations increase significantly.

The crawling speed varies depending on the detection zone height from approx. 0.1 to 0.4 m/s. At lower heights, crawling tends to be slower. Based on the main study, the crawling speed at  $H_{DB} \leq 300$  mm can be conservatively estimated at approx. 0.4 m/s to the safe direction.

In the preliminary study, the adult test subjects crawled more slowly on less favourable ground. Otherwise, the results were similar to those in the main study.

For comparison, the 10 adult participants were tested in a similar manner to determine the lateral ability to bypass of an invisible 3D detection zone. The distances to be bypassed between the boundary of a wall and the 3D detection zone showed no differences from the results for crawling beneath. The bypass speed is estimated to be higher, at a maximum of 0.6 m/s.

## 6 Summary and limits of application

This “Fachbereich AKTUELL” is based on expert knowledge gathered by the expert committee woodworking and metalworking, subcommittee machinery, robotics and automation of Deutsche Gesetzliche Unfallversicherung (DGUV) and findings from accidents in the field of machine safety. It has been developed in cooperation with the „Institut für Arbeitsschutz (IFA).

It is intended to support manufacturers of machinery and equipment in implementing the requirements for safeguarding hazardous areas by means of 3D ESPE.

The results of the investigations in accordance with chapter 5 represent no direct specification for the dimensioning of 3D detection zones in relation to the ground clearance.

In accordance with Annexes AA of DIN EN IEC 61496-3 and DIN IEC/TS 61496-4-3, system-specific properties such as random and systematic measurement errors of the respective 3D ESPE and algorithms for evaluating the object position can also be considered.

The provisions of individual laws and regulations remain unaffected by this "Fachbereich AKTUELL". The requirements of the statutory regulations apply without restriction.

To obtain complete information, it is necessary to consult the relevant regulatory texts.

This “Fachbereich AKTUELL” is the English translation of the German edition 1/2026. In any case, the German original shall prevail. No liability is accepted for translation errors.

The expert committee Woodworking and Metalworking is composed of representatives of the German accident insurance institutions, public bodies, social partners and manufacturing and operating companies.

Further "Fachbereich AKTUELL" or information sheets from the expert committee Woodworking and Metalworking (FBHM) are available for free download on the Internet [8].

## Bibliography

- [1] [DIN EN ISO 13855:2010-10](#); Sicherheit von Maschinen - Anordnung von Schutzeinrichtungen im Hinblick auf Annäherungsgeschwindigkeiten von Körperteilen; DIN Media GmbH, Berlin
- [2] [DIN EN ISO 13855:2025-10](#); Sicherheit von Maschinen - Anordnung von Schutzeinrichtungen im Hinblick auf Annäherung des menschlichen Körpers; DIN Media GmbH, Berlin
- [3] [DIN EN IEC 61496-3](#); [VDE 0113-203: 2019-10](#); Sicherheit von Maschinen - Berührungslos wirkende Schutzeinrichtungen - Teil 3: Besondere Anforderungen an aktive optoelektronische diffuse Reflektion nutzende Schutzeinrichtungen (AOPDDR); DIN Media GmbH, Berlin
- [4] [IEC 61496-3:2025-08](#) Safety of machinery - Electro-sensitive protective equipment - Part 3: Particular requirements for active opto-electronic protective devices responsive to diffuse reflection (AOPDDR); IEC, Genf
- [5] [DIN IEC/TS 61496-4-3](#); [VDE V 0113-204-3:2023-12](#); Sicherheit von Maschinen - Berührungslos wirkende Schutzeinrichtungen - Teil 4-3: Besondere Anforderungen an Einrichtungen, die bildverarbeitende Schutzeinrichtungen (VBPD) verwenden - Zusätzliche Anforderungen bei Verwendung von stereoskopischen Betrachtungsverfahren (VBPDST); DIN Media GmbH, Berlin
- [6] Safety and Usability through Applications in virtual Environments (SUTAVE)-Labor des IFA.
- [7] Hoyer, G.; Hauke, M.; Lungfiel, A.; Nickel, P.; Huelke, M.; Bömer, T.; Gestaltungsanforderungen an dreidimensionale Schutzräume für Fertigungszellen mit Mensch-Roboter-Interaktion - Eine Pilotstudie in virtueller Realität - Gestaltung nachhaltiger Arbeitssysteme - Wege zur gesunden, effizienten und sicheren Arbeit. 58. Kongress der Gesellschaft für Arbeitswissenschaft, 22.-24. Februar 2012, Kassel - Vortrag. Berichtsband und CD-ROM, S. 643-646, Hrsg.: Gesellschaft für Arbeitswissenschaft, GfA-Press, Dortmund 2012. ISBN: 978-3-936804-12-6
- [8] Internet: [www.dguv.de/fb-holzundmetall](http://www.dguv.de/fb-holzundmetall) oder Publikationen oder [www.bghm.de](http://www.bghm.de) Webcode: <626>

## Picture credits

- Figures 1, 3 – Roboter © beawolf/stock.adobe.com / Sonstiges © IFA
- Figures 2, 4 – Institut für Arbeitsschutz (IFA) der Deutschen Gesetzlichen Unfallversicherung DGUV, 53754 Sankt Augustin

### Imprint

Deutsche Gesetzliche  
Unfallversicherung e.V. (DGUV)  
Glinkastraße 40  
10117 Berlin  
Telefon: 030 13001-0 (Zentrale)  
E-Mail: [info@dguv.de](mailto:info@dguv.de)  
Internet: [www.dguv.de](http://www.dguv.de)

DGUV Expert Committee for Woodworking and  
Metalworking, subcommittee Machinery, Robotics  
and Automation

<https://www.dguv.de/fb-holzundmetall/index.jsp>

The DGUV expert committees are led by the German Social Accident Insurance Institutions for the Public Sector, the industry-related German Social Accident Insurance Institutions and the umbrella organisation DGUV. The German Social Accident Insurance Institution for the Woodworking and Metalworking Industries (BGHM) is the institution in charge for the expert committee Woodworking and Metalworking and thus the first point of contact at federal level for questions regarding the health and safety at work in this field. The following parties were involved in the development of this Fachbereich AKTUELL:

- Abteilung Unfallprävention: Digitalisierung – Technologien des Instituts für Arbeitsschutz der DGUV (IFA)
- Pilz GmbH & Co. KG, Product Development / Sensor Technology